Supplementary Information

Diverse tetracyanodihydrodipyradinopyradine clathrate crystals assembled from weak intermolecular interactions

Kosuke Watanabe,[a,b] Haruki Sugiyama[a,b,c,d] and Yasutomo Segawa*[a,b]

[a] *Institute for Molecular Science, Myodaiji, Okazaki, 444-8787, Japan*

[b] *The Graduate University for Advanced Studies, SOKENDAI, Myodaiji, Okazaki, 444-8787, Japan.*

[c] *Neutron Industrial Application Promotion Center, Comprehensive Research Organization for Science and Society, Tokai, Ibaraki 319-1106, Japan*

[d] *Department of Chemistry, School of Science, Institute of Science Tokyo, 2-12-1, Ookayama, Meguro, Tokyo, Japan*

E-mail: segawa@ims.ac.jp

Table of Contents

1. Experimental section

Single crystal X-ray diffraction measurements

Details of the crystal data and a summary of the intensity data collection parameters are listed in Table S4. Suitable crystals were mounted with mineral oil on a MiTeGen MicroMounts and transferred to the goniometer of the kappa goniometer of a RIGAKU XtaLAB Synergy Custom system with equipped with mirror monochromated Mo Kα radiation (λ = 0.71073 Å) and HyPix-6000HEIC detector or RIGAKU supernova equipped with mirror monochromated Cu Kα radiation (λ = 1.54184 Å) and EosS2 CCD detector. Cell parameters were determined and refined, and raw frame data were integrated using CrysAlisPro (Rigaku Oxford Diffraction, 2018). The structures were solved by dual methods using SHELXT[S1] and refined by full-matrix least-squares techniques against F^2 with SHELXL-2018/3[S2] using Olex2 software package.[S3] The intensities were corrected for Lorentz and polarization effects. All non-hydrogen atoms were refined with anisotropic displacement parameters. Hydrogen atoms were refined isotropically as riding model.

Powder X-ray diffraction (PXRD) measurements

PXRD data were recorded by using Rigaku MiniFlex 600-C diffractometer with Cu Kα, λ = 1.54184 Å or Rigaku SmartLab diffractometer with Cu Kα, λ = 1.54184 Å. The 2θ scans were performed with a step size of 0.01° and a speed of 5° min^{-1}, unless otherwise noted.

For comparison, PXRD pattern simulation was performed using the CIF file **HC-TCDP(r.t.)** obtained by single crystal X-ray diffraction and visualized using Mercury 2024.3.1 with a FWHM (Full Width at Half Maximum) value of 0.1°.

Thermogravimetric analysis (TG-DTA) measurements

TG-DTA data were recorded simultaneously on a Rigaku Thermo Plus EVO II TG8120 instrument. The samples were heated from room temperature to 250 °C at 10 °C/min under a dry nitrogen atmosphere (flow rate = 50 mL/min).

2. Computational study

Gaussian

The Gaussian 16 program[S4] running on a NEC LX 110Rh system was used for all calculations. Structures were optimized at B3LYP/6-31G(d).[S5,S6] Zero-point energy, enthalpy, and Gibbs free energy at 298.15 K and 1 atm were estimated from the gas-phase studies. Harmonic vibration frequency calculation at the same level was performed to verify all stationary points as local minima (with no imaginary frequency). Uncorrected and thermal-corrected energies of stationary points were shown in Table S1.

Table S1 Uncorrected and thermal-corrected (298 K) energies of stationary points (Hartree).[a]

	E	*E* + *ZPE*	*H*	*G*
TCDP	–1703.92138916	–1703.456075	–1703.417650	–1703.530864

a) *E*: electronic energy; *ZPE*: zero-point energy; *H* (= $E + ZPE + E_{vib} + E_{rot} + E_{trans} + RT$): sum of electronic and thermal enthalpies; *G* (= $H - TS$): sum of electronic and thermal free energies.

NCI plot

NCI plot[S7,S8] was calculated by a NCIPLOT 4.0 program using crystal structures of **TCDP·acetone** and **TCDP·MeCN**.

CrystalExplorer

CE-B3LYP was employed for all crystal data calculations using CrystalExplorer 21.3,[S9] which included energy decomposition analysis. The following equations 4.1 relate the E_{tot} to the E_{ele}, E_{pol}, E_{dis}, and E_{rep}. The scaling factor in the CE-B3LYP method is given in Table S2.

$$E_{tot} = k_{ele} \cdot E_{ele} + k_{pol} \cdot E_{pol} + k_{dis} \cdot E_{dis} + k_{rep} \cdot E_{rep} \qquad (4.1)$$

Table S2 Scaling factor in this calculation.

	k_{ele}	k_{pol}	k_{dis}	k_{rep}
CE-B3LYP	1.057	0.740	0.871	0.618

Table S3 Energy of interactions between a TCDP molecule and the most interacting TCDP or guest molecule.

kJ·mol^{-1}	interaction with	E_{ele}	E_{pol}	E_{dis}	E_{rep}	E_{tot}
TCDP·EtOAc	TCDP	–34.7	–8.8	–50.7	37.3	–64.3
	EtOAc*	–20.3	–6.7	–31.1	21.5	–40.2
TCDP·acetone	TCDP	–36.9	–10.9	–65.4	52.1	–71.8
	acetone	–19.6	–6.9	–26.5	22.7	–34.9
TCDP·benzene	TCDP	–27.3	–7.8	–32.3	21.1	–49.7
	benzene	–8.3	–3.2	–37.3	21.1	–30.6
TCDP·MeCN	TCDP	–33.0	–8.6	–40.7	39.6	–52.1
	MeCN	–16.0	–5.3	–12.0	14.8	–22.2
TCDP·DCE	TCDP	–30.2	–7.9	–37.5	30.4	–51.7
	DCE	–7.5	–1.4	–13.7	10.3	–14.6

* Average value from two crystallographically independent molecules.

3. X-ray crystallography

Table S4 Crystallographic data and structure refinement details of obtained crystals.

	TCDP·2EtOAc	**TCDP**·PhCl	**TCDP**·PhI
formura	$C_{30}H_{22}N_{10}·2(C_4H_8O_2)$	$C_{30}H_{22}N_{10}·C_6H_5Cl$	$C_{30}H_{22}N_{10}·C_6H_5I$
Fw	698.78	635.12	726.57
T (K)	143.15	143.15	143.15
λ (Å)	0.71073	0.71073	0.71073
cryst syst	Orthorhombic	Triclinic	Triclinic
space group	$Pna2_1$	P-1	P-1
a (Å)	26.3360(19)	8.1115(4)	8.1750(4)
b (Å)	9.3587(5)	8.9633(6)	9.1048(5)
c (Å)	15.4039(8)	11.3830(7)	11.3499(6)
α (deg)	90	82.417(5)	81.725(4)
β (deg)	90	78.205(5)	77.867(4)
γ (deg)	90	77.833(5)	76.129(4)
V (Å^3)	3796.6(4)	788.51(8)	797.93(7)
Z	4	1	1
D_{calc} (g·cm^{-1})	1.223	1.338	1.512
μ (mm^{-1})	0.083	0.165	1.047
F(000)	1472.0	330.0	366.0
cryst size (mm)	0.10 × 0.10 × 0.08	0.10 × 0.10 × 0.10	0.10 × 0.10 × 0.10
2θ range (deg)	5.960 to 54.190	4.670 to 54.202	5.630 to 54.198
reflns collected	16645	9331	8772
indep reflns/R_{int}	7049/0.0464	3480/0.0558	3512/0.0464
params	479	223	235
GOF on F^2	1.019	1.080	1.019
R_1, wR_2 [I>2σ(I)]	0.0530, 0.1135	0.0864, 0.2622	0.0517, 0.1290
R_1, wR_2 (all data)	0.0983, 0.1392	0.1132, 0.2888	0.0729, 0.1415
CCDC Number	2429929	2429930	2429931

	TCDP·2acetone	**TCDP**·2DMF	**TCDP**·2THF
formura	$C_{30}H_{22}N_{10}·2(C_3H_6O)$	$C_{30}H_{22}N_{10}·2(C_3H_7NO)$	$C_{30}H_{22}N_{10}·2(C_4H_8O)$
Fw	638.73	668.77	666.78
T (K)	143.15	200.15	143.15
λ (Å)	0.71073	1.54184	0.71073
cryst syst	Monoclinic	Monoclinic	Monoclinic
space group	$P2_1/n$	$P2_1/n$	$P2_1/n$
a (Å)	8.7836(4)	9.0545(2)	9.0161(4)
b (Å)	12.5914(5)	12.3215(3)	12.1980(6)
c (Å)	15.6251(9)	16.3699(3)	16.1054(7)
α (deg)	90	90	90
β (deg)	96.763(5)	92.908(2)	99.256(4)
γ (deg)	90	90	90
V (Å^3)	1716.08(14)	1823.96(7)	1748.18(14)
Z	2	2	2
D_{calc} (g·cm^{-1})	1.236	1.218	1.267
μ (mm^{-1})	0.081	0.652	0.083
F(000)	672.0	704.0	704.0
cryst size (mm)	0.10 × 0.10 × 0.10	0.10 × 0.08 × 0.08	0.10 × 0.03 × 0.03
2θ range (deg)	5.682 to 54.206	8.988 to 136.438	5.908 to 54.206
reflns collected	11316	6480	13406
indep reflns/R_{int}	3772/0.0716	330/0.0241	3855/0.0547
params	222	278	239
GOF on F^2	1.041	1.029	1.008
R_1, wR_2 [I>2σ(I)]	0.0623, 0.1608	0.0529, 0.1458	0.0591, 0.1201
R_1, wR_2 (all data)	0.0931, 0.1837	0.0606, 0.1565	0.0985, 0.1343
CCDC Number	2429932	2429933	2429934

	TCDP·4benzene	**TCDP**·4thiophene	**TCDP**·2Ph_2O
formura	$C_{30}H_{22}N_{10}\cdot4(C_6H_6)$	$C_{30}H_{22}N_{10}\cdot4(C_4H_4S)$	$C_{30}H_{22}N_{10}\cdot2(C_{12}H_{10}O)$
Fw	835.01	859.10	862.97
T (K)	200.15	143.15	143.15
λ (Å)	1.54184	0.71073	0.71073
cryst syst	Triclinic	Triclinic	Triclinic
space group	*P*-1	*P*-1	*P*-1
a (Å)	10.4303(7)	10.4879(5)	9.6542(6)
b (Å)	11.1097(10)	10.8573(5)	11.4847(10)
c (Å)	11.7866(10)	11.2117(5)	11.5991(9)
α (deg)	65.920(9)	68.012(4)	112.246(8)
β (deg)	69.939(7)	68.117(4)	95.182(6)
γ (deg)	85.587(7)	86.081(4)	103.220(7)
V (Å^3)	1168.12(19)	1094.75(10)	1136.23(17)
Z	1	1	1
D_{calc} (g·cm^{-1})	1.187	1.303	1.261
μ (mm^{-1})	0.566	0.263	0.080
F(000)	440.0	448.0	452.0
cryst size (mm)	0.05 × 0.03 × 0.03	0.15 × 0.15 × 0.15	0.05 × 0.05 × 0.20
2θ range (deg)	8.742 to 136.492	6.080 to 52.744	5.272 to 54.204
reflns collected	7472	13745	15682
indep reflns/R_{int}	4263/0.0331	4471/0.0454	5008/0.1057
params	292	274	301
GOF on F^2	0.990	1.076	1.194
R_1, wR_2 [$I>2\sigma(I)$]	0.0614, 0.1388	0.0997, 0.2865	0.1422, 0.2521
R_1, wR_2 (all data)	0.1042, 0.1705	0.1227, 0.3145	0.2316, 0.2901
CCDC Number	2429935	2429936	2429937

	TCDP·2pyridine	**TCDP**·DCM	**TCDP**·2DCE
formura	$C_{30}H_{22}N_{10}\cdot2(C_5H_5N)$	$C_{30}H_{22}N_{10}\cdot CH_2Cl_2$	$C_{30}H_{22}N_{10}\cdot2(C_2H_4Cl_2)$
Fw	680.77	607.50	720.48
T (K)	143.15	143.15	143.15
λ (Å)	1.54184	0.71073	0.71073
cryst syst	Triclinic	Monoclinic	Monoclinic
space group	*P*-1	*C*2/*c*	$P2_1/c$
a (Å)	9.3409(8)	14.1431(5)	12.2866(4)
b (Å)	12.7905(11)	9.8855(3)	8.6175(3)
c (Å)	16.1963(14)	22.1824(12)	16.7215(5)
α (deg)	70.868(8)	90	90
β (deg)	83.072(7)	106.036(4)	90.982(3)
γ (deg)	82.513(7)	90	90
V (Å^3)	1806.3(3)	2980.7(2)	1770.21(10)
Z	2	4	2
D_{calc} (g·cm^{-1})	1.252	1.354	1.352
μ (mm^{-1})	0.630	0.258	0.375
F(000)	712.0	1256.0	744.0
cryst size (mm)	0.15 × 0.08 × 0.02	0.10 × 0.05 × 0.05	0.10 × 0.10 × 0.02
2θ range (deg)	5.796 to 136.502	5.096 to 54.206	4.872 to 50.692
reflns collected	6592	14879	13167
indep reflns/R_{int}	6592/-	3278/0.0280	3239/0.0242
params	476	211	237
GOF on F^2	1.072	1.021	1.040
R_1, wR_2 [$I>2\sigma(I)$]	0.0787, 0.2206	0.0492, 0.1203	0.0412, 0.1034
R_1, wR_2 (all data)	0.1146, 0.2491	0.0634, 0.1277	0.0479, 0.1073
CCDC Number	2429938	2429939	2429940

	TCDP·2MeCN	**TCDP**·PhMe	**TCDP**·ODCB
formura	$C_{30}H_{22}N_{10}·2(C_2H_3N)$	$C_{30}H_{22}N_{10}·C_7H_8$	$C_{30}H_{22}N_{10}·C_6H_4Cl_2$
Fw	604.68	614.71	669.57
T (K)	143.15	143.15	143.15
λ (Å)	0.71073	0.71073	0.71073
cryst syst	Monoclinic	Monoclinic	Monoclinic
space group	$P2_1/c$	$P2_1/c$	$P2_1/c$
a (Å)	11.1575(5)	11.6712(2)	11.7987(4)
b (Å)	8.9502(4)	18.7282(3)	19.0987(4)
c (Å)	16.0650(8)	24.0317(5)	23.8997(6)
α (deg)	90	90	90
β (deg)	90.969(4)	103.377(2)	103.244(3)
γ (deg)	90	90	90
V (Å^3)	2137.7(2)	5110.35(15)	5242.3(3)
Z	2	6	6
D_{calc} (g·cm^{-1})	1.252	1.198	1.273
μ (mm^{-1})	0.080	0.075	0.227
F(000)	632.0	1932.0	2076.0
cryst size (mm)	0.10 × 0.10 × 0.10	0.15 × 0.10 × 0.08	0.10 × 0.10 × 0.10
2θ range (deg)	5.836 to 54.200	4.212 to 55.756	4.868 to 54.204
reflns collected	10328	58548	53311
indep reflns/R_{int}	3549/0.0318	12179/0.0329	11561/0.0588
params	212	791	670
GOF on F^2	1.074	1.021	1.050
R_1, wR_2 [$I>2\sigma(I)$]	0.0441, 0.1089	0.0502, 0.1309	0.0775, 0.2194
R_1, wR_2 (all data)	0.0624, 0.1184	0.0625, 0.1382	0.1134, 0.2429
CCDC Number	2429941	2429942	2429943

	HC-TCDP	**HC-TCDP**(room temperature)
formura	$C_{30}H_{22}N_{10}$	$C_{30}H_{22}N_{10}$
Fw	522.57	522.57
T (K)	143.15	293.15
λ (Å)	0.71073	1.54184
cryst syst	Triclinic	Triclinic
space group	P-1	P-1
a (Å)	8.1539(6)	8.2859(7)
b (Å)	8.5097(5)	8.7094(9)
c (Å)	10.9361(11)	11.0860(9)
α (deg)	101.144(7)	102.350(8)
β (deg)	101.548(7)	100.096(7)
γ (deg)	102.714(6)	105.742(8)
V (Å^3)	702.52(10)	728.67(12)
Z	1	1
D_{calc} (g·cm^{-1})	1.235	1.191
μ (mm^{-1})	0.079	0.610
F(000)	272.0	272.0
cryst size (mm)	0.04 × 0.04 × 0.01	0.08 × 0.02 × 0.02
2θ range (deg)	5.066 to 52.744	10.980 to 143.054
reflns collected	6796	4979
indep reflns/R_{int}	2863/0.0437	2756/0.0231
params	184	184
GOF on F^2	1.019	1.050
R_1, wR_2 [$I>2\sigma(I)$]	0.0475, 0.1097	0.0619, 0.1548
R_1, wR_2 (all data)	0.0954, 0.1275	0.0992, 0.1805
CCDC Number	2429944	2431197

(CCDC = Cambridge crystallographic data centre, Fw = formula weight, cryst syst = crystal system, reflns = reflections, indep = independent, GOF = good of fit)

Table S5 Summary of the obtained clathrate crystals.

Solvent	Host network frameworks	Host network	host/guest	Space group
EtOAc	π-π host networks	1D	1/2	$Pna2_1$
PhCl	π-π host networks	1D	1/1	*P*-1
PhI	π-π host networks	1D	1/1	*P*-1
acetone	π-π host networks	2D	1/2	$P2_1/n$
DMF	π-π host networks	2D	1/2	$P2_1/n$
THF	π-π host networks	2D	1/2	$P2_1/n$
Ph_2O	π-π host networks	2D	1/2	*P*-1
benzene	π-π host networks	2D	1/4	*P*-1
thiophene	π-π host networks	2D	1/4	*P*-1
pyridine	π-π host networks	3D	1/2	*P*-1
DCM	π-π host networks	3D	1/1	*C*2/*c*
DCE	CN-π host networks	2D	1/2	$P2_1/c$
MeCN	CN-π host networks	2D	1/2	$P2_1/c$
PhMe	CN-π host networks	3D	1/1	$P2_1/c$
ODCB	CN-π host networks	3D	1/1	$P2_1/c$

4. Exposure experiments

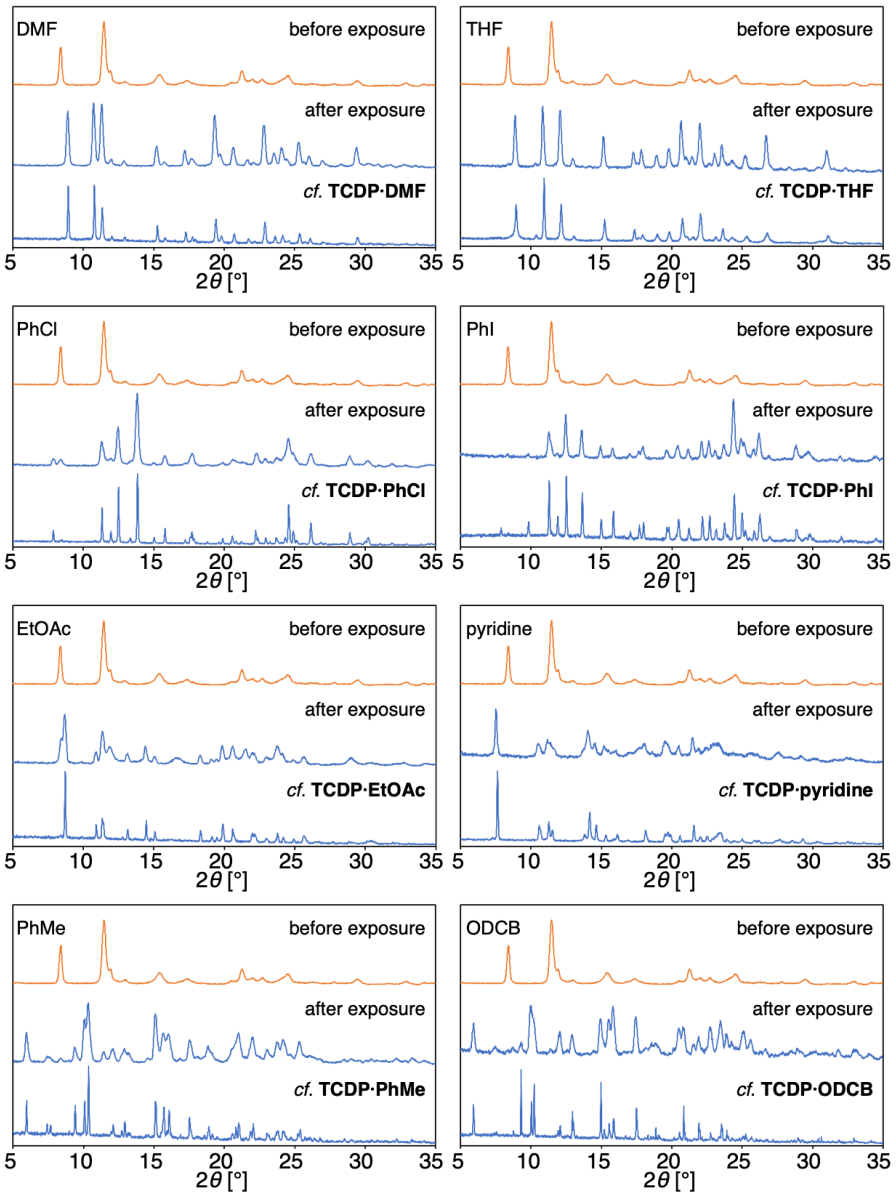

Fig. S1 Results of the solvent vapor exposure experiment.

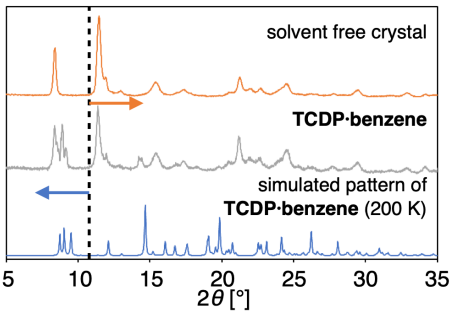

Fig. S2 Desorption behavior of **TCDP·benzene**. The 2θ scans were performed with a step size of 0.01° and a speed of 1° min^{-1}.

5. Desorption tracking by TG-DTA

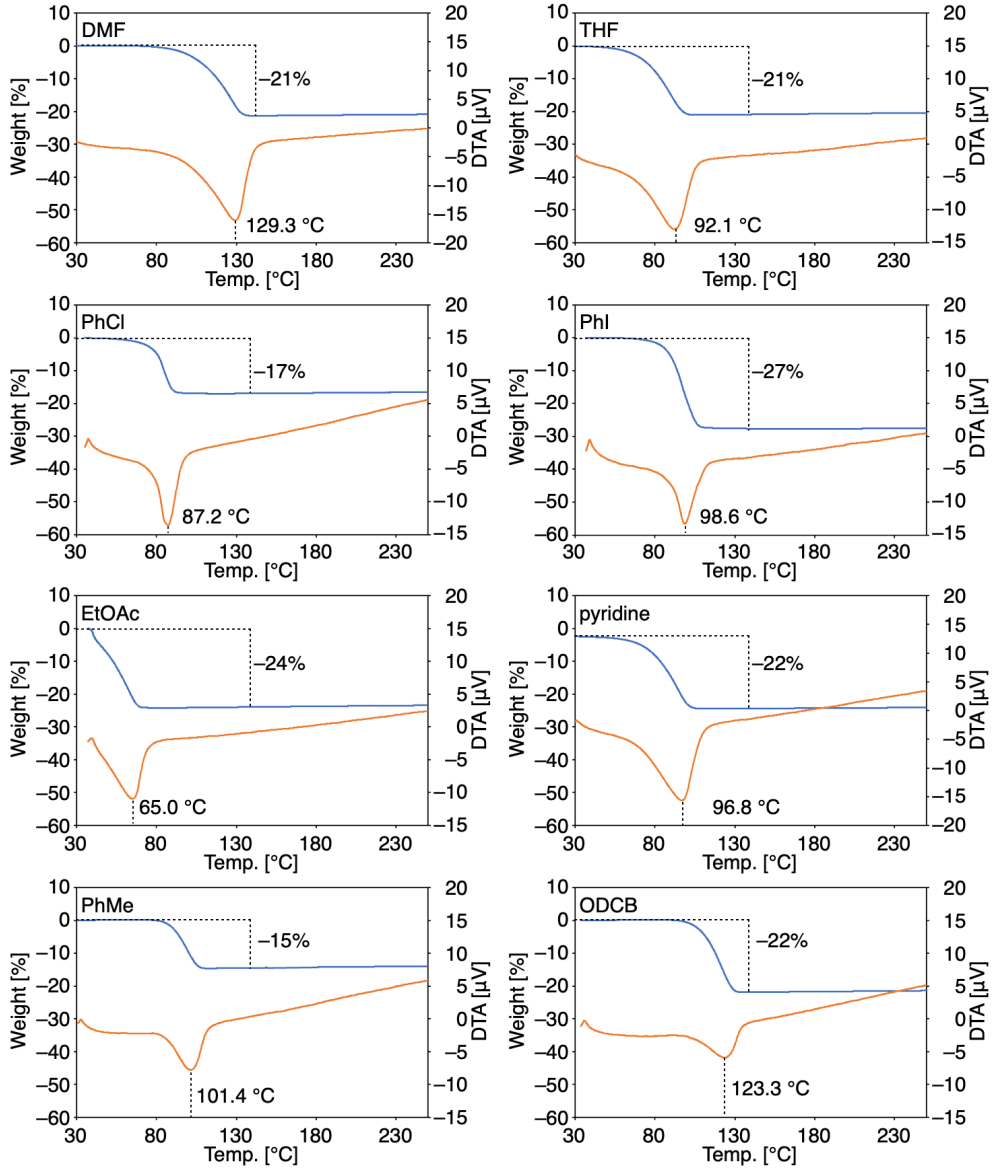

Fig. S3 TG-DTA curves of corresponding clathrate crystals.

Table S6 Summary of TG-DTA analysis.

solvent	host/guest ratio	formula weight	desorption temp. (°C)	decrease (calcd., %)	decrease (obs., %)	error (%)
PhCl	1/1	635.14	87.2	–17.72	–16.93	0.79
PhI	1/1	726.59	98.6	–28.08	–27.42	0.66
EtOAc	1/2	698.80	65.0	–25.22	–24.09	1.13
acetone	1/2	638.74	92.4	–18.19	–17.44	0.75
DMF	1/2	668.78	129.3	–21.86	–21.23	0.63
THF	1/2	666.80	92.1	–21.63	–20.83	0.80
pyridine	1/2	680.78	96.8	–23.24	–22.05	1.19
MeCN	1/2	604.68	78.5	–13.58	–12.59	0.99
PhMe	1/1	614.72	101.4	–14.99	–14.67	0.32
ODCB	1/1	669.58	123.3	–21.95	–21.84	0.11

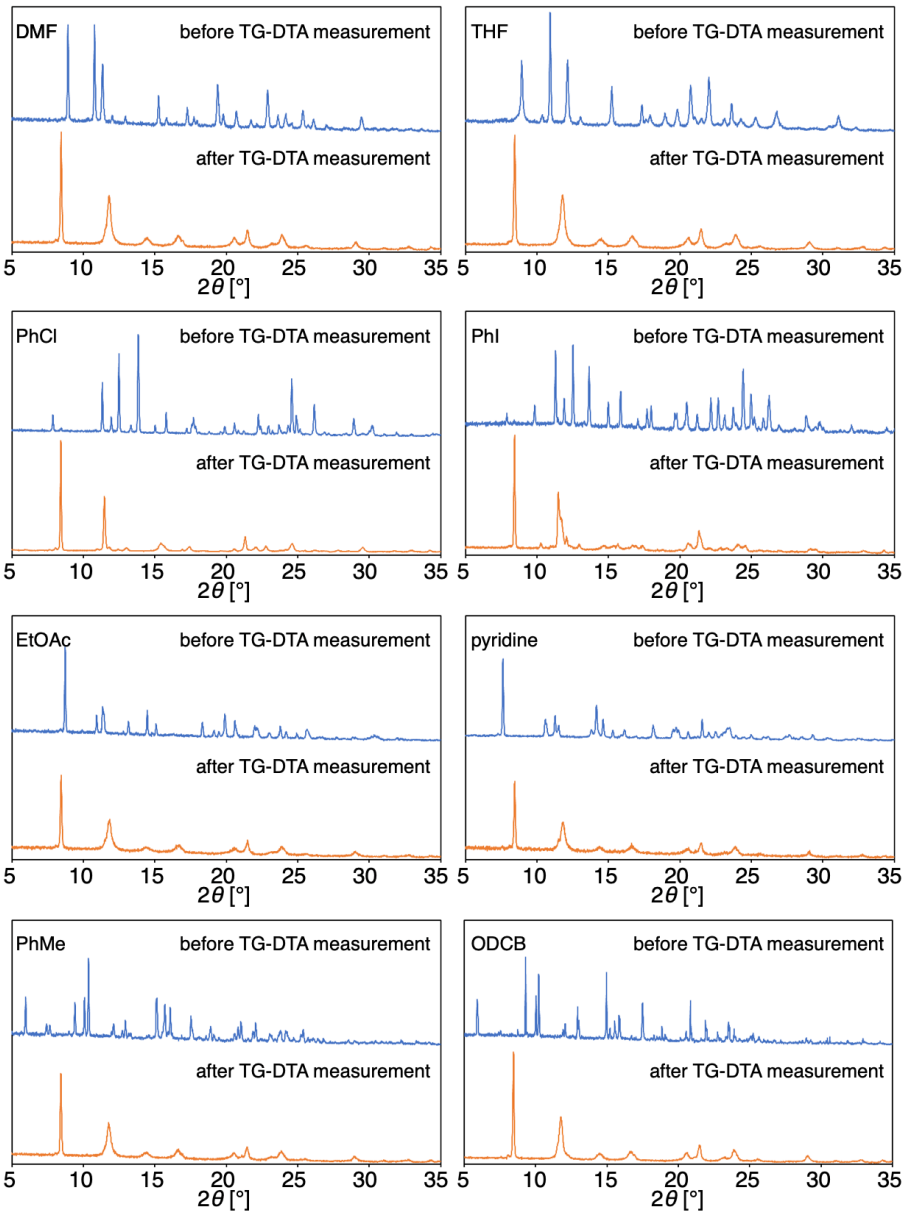

Fig. S4 PXRD pattern before and after TG-DTA measurement.

6. Desorption tracking by PXRD

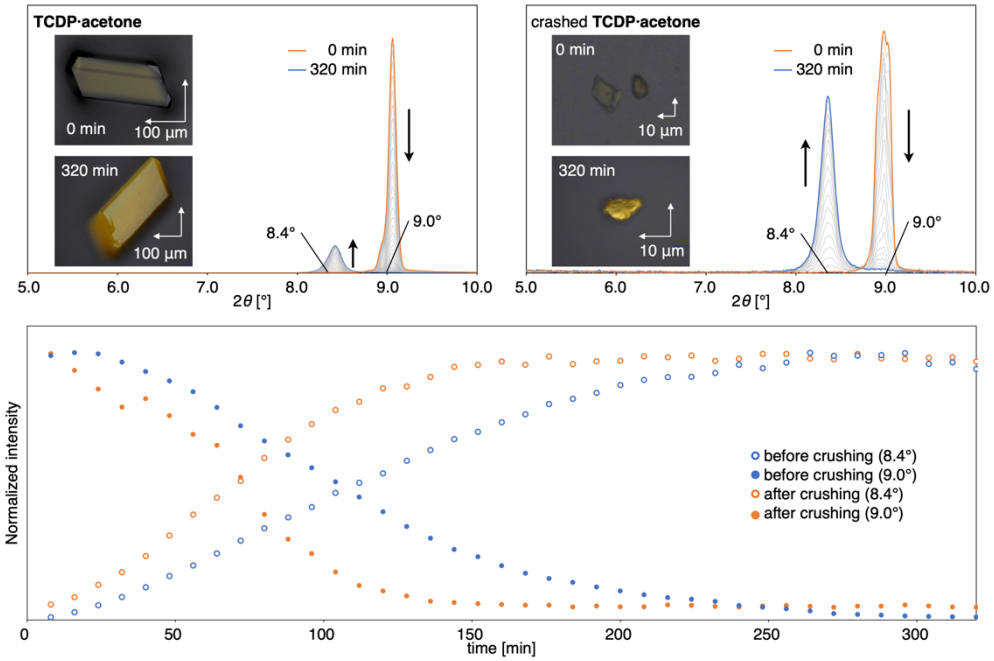

Fig. S5 (a) Time-dependent PXRD analysis of intact (top-left) and crushed (top-right) **TCDP·acetone**, and evolution of peak intensity at 8.4° and 9.0° (bottom). Measurements were performed every 8 minutes, at room temperature and under atmospheric conditions.

7. References

[S1] G. M. Sheldrick, *Acta Crystallogr*., 2015, **A71**, 3–8.

[S2] G. M. Sheldrick, *Acta Crystallogr*., 2015, **C71**, 3–8.

[S3] O. V Dolomanov, L. J. Bourhis, R. J. Gildea, J. A. K. Howard and H. Puschmann, *J. Appl. Crystallogr.,* 2009, **42**, 339–341.

[S4] M. J. Frisch, G. W. Trucks, H. B. Schlegel, G. E. Scuseria, M. A. Robb, J. R. Cheeseman, G. Scalmani, V. Barone, G. A. Petersson, H. Nakatsuji, X. Li, M. Caricato, A. V. Marenich, J. Bloino, B. G. Janesko, R. Gomperts, B. Mennucci, H. P. Hratchian, J. V. Ortiz, A. F. Izmaylov, J. L. Sonnenberg, D. Williams-Young, F. Ding, F. Lipparini, F. Egidi, J. Goings, B. Peng, A. Petrone, T. Henderson, D. Ranasinghe, V. G. Zakrzewski, J. Gao, N. Rega, G. Zheng, W. Liang, M. Hada, M. Ehara, K. Toyota, R. Fukuda, J. Hasegawa, M. Ishida, T. Nakajima, Y. Honda, O. Kitao, H. Nakai, T. Vreven, K. Throssell, J. A. Montgomery, Jr., J. E. Peralta, F. Ogliaro, M. J. Bearpark, J. J. Heyd, E. N. Brothers, K. N. Kudin, V. N. Staroverov, T. A. Keith, R. Kobayashi, J. Normand, K. Raghavachari, A. P. Rendell, J. C. Burant, S. S. Iyengar, J. Tomasi, M. Cossi, J. M. Millam, M. Klene, C. Adamo, R. Cammi, J. W. Ochterski, R. L. Martin, K. Morokuma, O. Farkas, J. B. Foresman and D. J. Fox, Gaussian 16, Revision C.02, Gaussian, Inc., Wallingford CT, 2016.

[S5] A. D. Becke, *J. Chem. Phys.,* 1993, **98**, 5648–5652.

[S6] C. Lee, W. Yang and R. G. Parr, *Phys. Rev. B,* 1988, **37**, 785–789.

[S7] E. R. Johnson, S. Keinan, P. Mori-Sánchez, J. Contreras-García, A. J. Cohen and W. Yang, *J. Am. Chem. Soc.*, 2010, **132**, 6498–6506.

[S8] J. Contreras-García, E. R. Johnson, S. Keinan, R. Chaudret, J.-P. Piquemal, D. N. Beratan and W. Yang, *J. Chem. Theory Comput.*, 2011, **7**, 625–632.

[S9] P. R. Spackman, M. J. Turner, J. J. McKinnon, S. K. Wolff, D. J. Grimwood, D. Jayatilaka and M. A. Spackman, *J. Appl. Crystallogr.*, 2021, **54**, 1006–1011.